Modeling of the Recrystallization and Austenite Formation Overlapping in Cold-Rolled Dual-Phase Steels During Intercritical Treatments

M. OLLAT, V. MASSARDIER, D. FABREGUE, E. BUSCARLET, F. KEOVILAY, and M. PEREZ

Austenite formation kinetics of a DP1000 steel was investigated from a ferrite–pearlite microstructure (either fully recrystallized or cold-rolled) during typical industrial annealing cycles by means of dilatometry and optical microscopy after interrupted heat treatments. A marked acceleration of the kinetics was found when deformed ferrite grains were present in the microstructure just before austenite formation. After having described the austenite formation kinetics without recrystallization and the recrystallization kinetics of the steel without austenite formation by simple JMAK laws, a mixture law was used to analyze the kinetics of the cold-rolled steel for which austenite formation and recrystallization may occur simultaneously. In the case where the interaction between these two phenomena is strong, three main points were highlighted: (i) the heating rate greatly influences the austenite formation kinetics, as it affects the degree of recrystallization at the austenite start temperature; (ii) recrystallization inhibition above a critical austenite fraction accelerates the austenite formation kinetics; (iii) the austenite fractions obtained after a 1 hour holding deviate from the local equilibrium fractions given by Thermo-Calc, contrary to the case of the recrystallized steel. This latter result could be due to the fact that the dislocations of the deformed ferrite matrix could promote the diffusion of the alloying elements of the steel and accelerate austenite formation.

DOI: 10.1007/s11661-017-4231-6

I. INTRODUCTION

DUAL-PHASE Steels (DP steels) are one of the most used Advanced High Strength Steels. This is due to the fact that their microstructures combining a ferritic matrix and martensite islands leads to a very good compromise between strength and ductility. In the case of cold-rolled steels, this type of microstructure is obtained by continuous annealing: an intercritical annealing (performed between Ac_1 and Ac_3) is followed by a rapid cooling, so that austenite transforms into martensite. The parameters (heating rate (R_H), annealing time and temperature) of the heating and holding stages play a major role on the final properties of DP steels, as they control the austenite fraction, the austenite grain size, and the carbon content of austenite at the end of the annealing treatment, before the quench.

During the first part of the treatment of DP steels, from a cold-rolled ferrite–pearlite microstructure, several microstructural evolutions are expected to occur more or less simultaneously depending on the applied parameters for the heating and soaking stages. This makes the understanding and modeling of microstructural evolutions during these stages rather difficult.

First, the cold-rolled ferrite matrix starts to recrystallize during the heating stage. A full recrystallization before reaching the austenite start temperature is assumed to be obtained only at very slow heating rates (<<5 K/s).[1,2] In most cases, recrystallization will not be finished when austenite formation becomes effective, leading to a possible interaction between recrystallization and austenite formation.[3]

Concomitant with recrystallization, cementite spheroidization takes place during the heating and holding stages. For example, Yang *et al.*[3] showed that cementite spheroidization occurs after a very short treatment time (20 seconds) at 973 K (700 °C). These observations were confirmed by other authors[2,4] who highlighted the presence of spheroidized cementite at the beginning of the transformation. This rapid

---

M. OLLAT is with Univ. Lyon INSA Lyon - MATEIS UMR CNRS 5510, 69621 Villeurbanne, France and also with the Fives Keods, 108-112 Avenue de la liberté, 94700 Maisons-Alfort, France. Contact e-mail: melanie.ollat@insa-lyon.fr V. MASSARDIER, D. FABREGUE, and M. PEREZ are with the Univ. Lyon INSA Lyon - MATEIS UMR CNRS 5510. E. BUSCARLET and F. KEOVILAY are with the Fives Keods, 108-112 Avenue de la liberté, 94700 Maisons-Alfort, France.

Manuscript submitted March 15, 2017.

spheroidization seems to be due to cementite fragmentation during cold rolling which introduces several defects (vacancies, dislocations).[5,6] This metallurgical phenomenon is important to consider as the austenite formation kinetics has been shown to be delayed when cementite spheroidized before austenite formation.[9]

Lastly, the third phenomenon to consider is austenite formation. Speich *et al.*[8] divided austenite formation from a ferrite–pearlite microstructure into three steps: (i) quick nucleation and growth managed by carbide dissolution, (ii) slower growth controlled by carbon diffusion in austenite and Mn diffusion in ferrite, and lastly (iii) slow equilibration of phases limited by Mn diffusion in austenite.

The interaction between recrystallization and austenite formation has been widely reported by several authors.[2–4,7,9–14] It is expected to be particularly strong at high heating rates.[12,14] In this case, recrystallization is shifted towards higher temperatures, which promotes the overlapping of recrystallization and austenite formation.

From a microstructural point of view, it has been clearly shown that a "strong interaction" (*i.e.,* a high heating rate) leads to a coarse microstructure with non-homogeneous ferrite/martensite repartition,[7,9,11,12] resulting from the fact that austenite nucleates and grows in parallel or before recrystallization. By contrast, a weak interaction is generally associated with a fine and homogeneous final microstructure.

From a kinetics point of view, several authors emphasized that recrystallization kinetics and austenite formation kinetics are influenced by their respective interaction. Yang *et al.*[3] and Ogawa *et al.*[13] clearly showed that recrystallization is not affected by austenite formation as long as austenite fraction is lower than 10 pct. By contrast, it could be substantially delayed[10,12] or blocked[14] above a critical austenite fraction (~10 to 30 pct). Two explanations were proposed for the recrystallization inhibition: (i) newly formed austenite may (partially) relax elastic energy stored in deformed ferrite grains (through crystal variants leading to a lowering of the local elastic stress fields), hence lowering the driving force for recrystallization nucleation; (ii) stabilization of deformed structures acting as long-distance diffusion paths for austenite formation. With regard to austenite formation, it seems to be greatly favored in deformed ferrite grains where the energy stored during cold rolling could increase the driving force for the transformation.[4]

The understanding of the interaction is a topic of interest. At the present time, modeling efforts remain very restricted. Some mesoscale approaches (including cellular automaton[15] and phase field[16]) have been proposed but quicker and simpler models are more relevant for industrial environment (for example, for online application). Kulakov *et al.*[17] proposed such an approach enabling the prediction of ferrite recrystallization and austenite formation in a DP900. However, these authors mentioned that the complex case where interaction occurs is difficult to model because the austenite formation kinetics is a function of the degree of recrystallization advancement.

In the above-mentioned context, the aim of the present paper is to develop a simple empirical model allowing the austenite formation kinetics of cold-rolled DP1000 steels to be predicted during typical industrial continuous annealing cycles. To reach this goal, a gradual approach has been adopted. First, the austenite formation kinetics of the steel has been studied, under non-isothermal and isothermal conditions, after full recrystallization of its ferritic matrix below Ac_1, in order to analyze austenite formation when recrystallization is absent. Second, recrystallization has been monitored before any austenite formation. Then, the more complex case of the cold-rolled DP steel for which austenite formation and recrystallization may interact, was considered.

From a theoretical point of view, the austenite formation kinetics in recrystallized ferrite and the recrystallization kinetics without austenite formation could be described by Johnson–Mehl–Avrami–Kolmogorov (JMAK) laws. Taking into account these results, the austenite formation kinetics of the investigated cold-rolled DP steel was analyzed with a simple mixture law assuming that the two different kinetics have to be considered for austenite nucleation and growth in deformed ferrite grains and in recrystallized ferrite grains. The present paper aims at discussing the results given by this simple approach under various conditions (continuous heating from room temperature to 1273 K (1000 °C) with different heating rates or heating followed by an isothermal holding at different temperatures).

II. MATERIAL AND EXPERIMENTAL PROCEDURE

A. *Material*

The present work was conducted on an industrially manufactured steel. After reheating and hot rolling in the austenitic domain, this steel was coiled at 903 K (630 °C) and cold-rolled with a 55 pct reduction ratio to produce sheets 1.5 mm thick. Its chemical composition, typically used for the production of DP1000 steels, is given in Table I.

In order to highlight the effect of the deformation on the austenite formation kinetics, two different initial states of the steel were considered in this study: (i) the initial cold-rolled state which is composed of a banded and strongly deformed ferrite–pearlitic microstructure and (ii) a fully recrystallized state which was obtained by an annealing treatment of 1200 seconds at 973 K (700 °C). In the following, the cold-rolled steel will be called "CR-steel" and the recrystallized steel "ReX-steel". Figure 1 shows the cold-rolled and recrystallized microstructures of the steel. The efficiency of the recrystallization treatment was confirmed by the presence of equiaxed ferrite grains and bands of spheroidized cementite.

Table I. Chemical Composition of the DP 1000 Steel Investigated in this Work

Element	C	Mn	Cr	Si	Al
Content (Wt Pct)	0.17	1.76	0.42	0.34	0.03
Content (At. Pct)	0.73	1.83	0.46	0.64	0.07

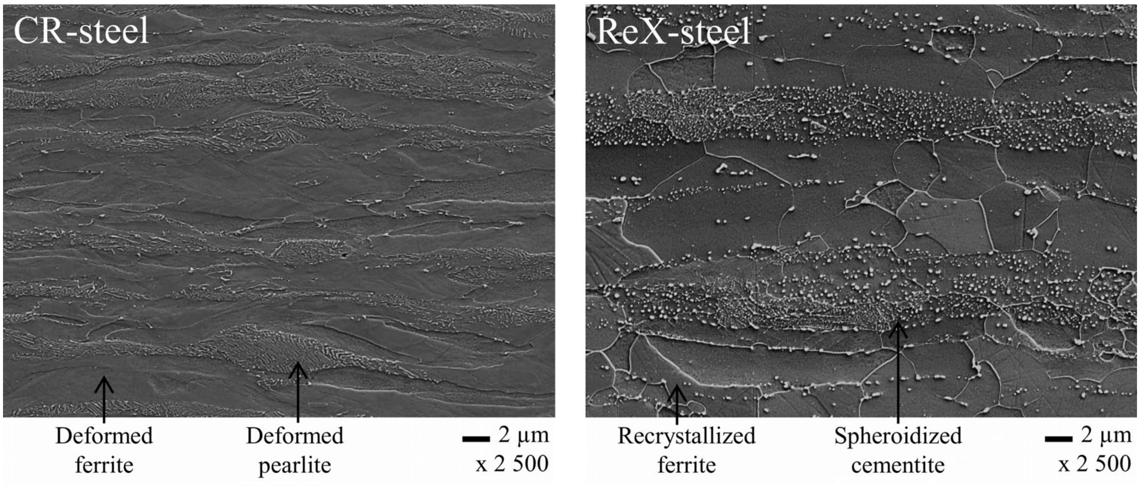

(a) (b)

Fig. 1—SEM micrographs of the two initial states of the steel: (*a*) cold-rolled state composed of a mixture of deformed bands of ferrite and pearlite; (*b*) recrystallized state characterized by equiaxed ferrite grains with bands of spheroidized cementite.

B. *Thermal Treatments*

Thermal treatments were performed in a *Gleeble 3500*[18] thermo-mechanical simulator using heating by Joule effect and cooling through direct water projection on the specimens. Samples (10 mm wide by 100 mm long) were treated with a precise temperature control (±3 K) thanks to the use of type-K thermocouples welded on the surface of the specimens.

For the thermal cycles including a heating stage followed by an isothermal holding at a given annealing temperature, the annealing was interrupted by rapid water cooling after different treatment times in order to follow the microstructural evolutions with time at the considered annealing temperature. In this work, the heating rate (R_H) was varied between 0.5 and 30 K/s to show its influence on the kinetics. Intercritical treatments were performed in the temperature range 993 K to 1053 K (720 °C to 780 °C) with annealing times inferior to 1 hour, in order to simulate typical industrial continuous annealing cycles.

C. *Experimental Procedure*

1. *Austenite formation kinetics*

The austenite formation kinetics of the CR-steel and of the ReX-steel were experimentally obtained by means of dilatometry. This technique is based on the monitoring of the change in the length of the samples during the thermal cycle. The dilatometer used for the experiment was an optical dilatometer set up on a *Gleeble* machine. The optical system allows a non-contact measurement of the length change in the alignment of thermocouples and avoids any dilatometer stress on the sample. The classical lever rule was used to monitor the austenite fraction during continuous heating from room temperature to 1273 K (1000 °C) for various heating rates.

The austenite fraction was also quantified by optical microscopy after treatments which were interrupted by a water quench, to transform austenite into martensite. On the corresponding samples, a Bandoh etching (2.3 mL Metabisulfite, 2.3 mL Picral, and 1 mL Nital) was used to differentiate ferrite from martensite. The quantification was performed at quarter thickness and by the average of 20 analyzed micrographies using *ImageJ* software.[19]

It should be noticed that the error bars for austenite fractions were fixed to 10 pct as the austenite fractions were evaluated by phase quantification on optical micrographs where errors may come from various sources (chemical etching, analysis of micrographs, threshold).

2. *Recrystallization kinetics*

In order to determine the isothermal recrystallization kinetics of ferrite, Vickers hardness measurements were performed on the CR-steel rapidly heated up to different temperatures within the range 923 K to 973 K (650 °C to 700 °C), below the austenite start temperature of the steel. For each treatment, about 15 measurements were performed at quarter thickness and with a 0.5 kg load.

3. *Microstructural characterization*

The microstructural changes induced by the different thermal treatments were analyzed by SEM observations conducted on a *Zeiss Supra 55 VP SEM* with an accelerating voltage of 10 kV. The samples for SEM observations were etched with a flash Nital (2 pct) after a standard grinding procedure to 0.06 μm.

D. *Thermodynamic Database*

In addition to experimental results, the austenite volume fraction was calculated from Thermo-Calc[20] using the TCFE8 Steels database.[21] Three equilibrium conditions were differentiated:

1. the orthoequilibrium (ORTHO) condition: it assumes that the thermodynamic equilibrium is reached for all elements. This type of equilibrium requires long treatment times.[22]
2. the paraequilibrium (PARA) condition: it supposes a constraint equilibrium without partitioning of substitutional alloying elements, *i.e.*, only C is at equilibrium, as defined by Hultgren.[23]
3. the local equilibrium (LE) of the ternary system Fe-0.17C-1.763Mn (wt pct) supposing a local equilibrium of C and Mn at the interface.[12,21] The newly formed austenite has the same Mn composition as the parent ferritic phase.[24,25] However a "spike" of Mn is created in order to satisfy the local equilibrium at the interface for both C and Mn. As highlighted by Chbihi *et al.*,[12] the LE condition applied for the $\alpha \rightarrow \gamma$ transformation is different from the LENP (Local Equilibrium with Negligible Partitioning) classically used in the $\gamma \rightarrow \alpha$ case.[26,27] From a practical point of view, LE fraction at a given temperature was calculated from the tie-line of the Fe-C-Mn ternary system for which the manganese content in austenite is equal to the one of the bulk material (*i.e.*, here 1.763 wt pctMn).

In these two last cases, the equilibrium is metastable and tends to reach the orthoequilibrium. In the case of the industrial thermal cycles considered in this work (times are short (less than 1 hour)), the conditions defining the orthoequilibrium are probably very difficult to reach especially at low temperature, as the diffusion of substitutional elements (such as Mn) is a limiting factor. To obtain a complete manganese redistribution in phases, it is generally admitted that several hours are required.[9]

III. RESULTS

A. *Preliminary Work: Non-isothermal Austenite Formation Kinetics Obtained by Dilatometry*

Figure 2 shows the non-isothermal austenite formation kinetics obtained by optical dilatometry on the ReX-steel and on the CR-steel during continuous heating from room temperature to 1273 K (1000 °C) at different heating rates. The ORTHO, PARA, and LE austenite volume fractions, calculated with Thermo-Calc, were also plotted. While the ORTHO and PARA austenite fractions are quite similar at low temperatures [below 1008 K (735 °C)], they tend to be notably different at higher temperatures. The deviation between the thermodynamic database and the non-isothermal experimental austenite formation kinetics is linked to the fact that the thermodynamic equilibrium is not achieved during continuous heating conditions—even at the lower heating rate 0.5 K/s. The diffusion of substitutional elements is so slow that more time is required to achieve the equilibrium condition.

In the case of the ReX-steel, the austenite formation kinetics is regularly shifted to higher temperature when the heating rate is increased, suggesting that austenite formation is a thermally activated phenomenon governed by a measurable activation energy. By contrast, on the CR-steel, the austenite formation kinetics is all superimposed and no clear evolution of the kinetics with the heating rate can be highlighted, supporting the idea that austenite formation could be strongly influenced by an interaction with recrystallization.

Figure 3 compares, for three heating rates, the austenite formation kinetics of the CR-steel and that of the ReX-steel. At very low heating rate (R_H = 0.5 K/s), the kinetics for austenite formation on CR-steel and ReX-steel is superimposed. For higher heating rate, the kinetics of the CR-steel tends to be accelerated compared to that of the ReX-steel and the acceleration appears to be all the more pronounced as the heating rate is increased. This tends to indicate that the presence of deformed ferrite grains in the CR-steel could play a major role on the austenite formation kinetics, as was already suggested by different authors.[4,12] Namely, non-recrystallized ferrite grains could promote austenite nucleation, as the energy stored in these grains during cold rolling could increase the driving force for austenite formation. Moreover, the higher fraction of deformed ferrite grains may also increase the number of austenite nucleation sites as suggested by Ogawa *et al.* [28]

It is also important to note that the degree of cementite spheroidization before austenite nucleation could also play a role in the kinetics. This effect will be discussed later in Section IV–A.

As already explained in the introduction of this paper, the main objective of the present works is to develop a simple model allowing the austenite formation kinetics of the CR-steel to be predicted. Due to the possible interaction between austenite formation and recrystallization in the intercritical domain, a progressive approach was chosen before treating this complex case. This is why, in a first step, the austenite formation kinetics of the ReX-steel (when recrystallization is absent) was investigated. Then, the recrystallization kinetics of the CR-steel was analyzed and modeled when no austenite formation occurs (that is to say, below the A_{C1} temperature). Lastly, the austenite formation kinetics of the CR-steel was analyzed.

B. *Austenite Formation Kinetics Without Recrystallization*

In order to model the non-isothermal austenite formation kinetics of the ReX-steel shown in Figure 2(a), the Johnson–Mehl–Avrami–Kolmogorov (JMAK) law was used in its differential form, *i.e.*,[29–31]:

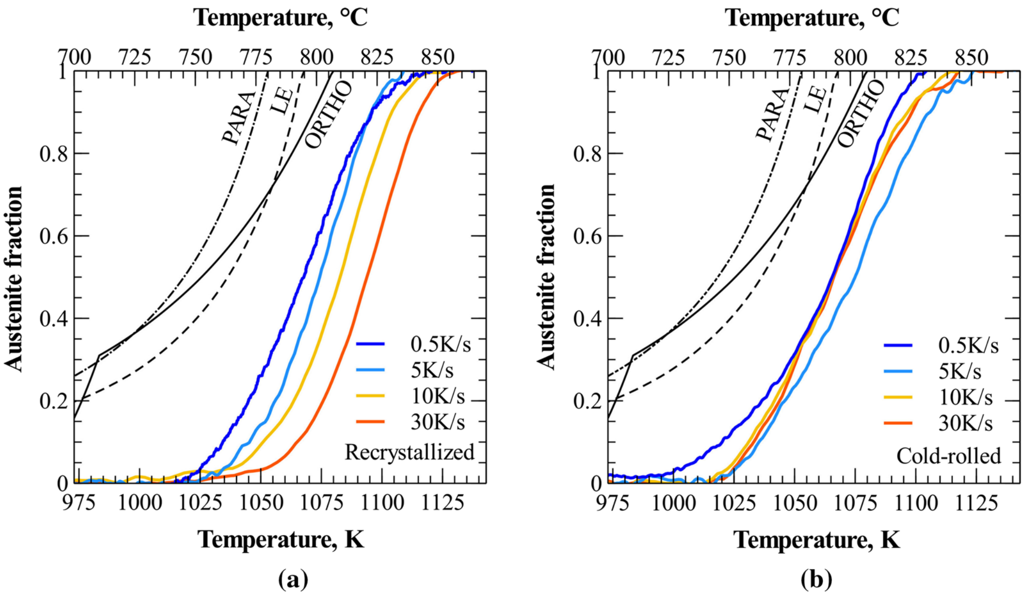

Fig. 2—Austenite formation kinetics obtained by dilatometry on the: (*a*) ReX-steel and (*b*) CR-steel during continuous heating from room temperature to 1273 K (1000 °C) with various heating rates R_H from 0.5 to 100 K/s. The ORTHO, PARA, and LE curves correspond, respectively to the orthoequilibrium, paraequilibrium, and local equilibrium conditions calculated from Thermo-Calc.

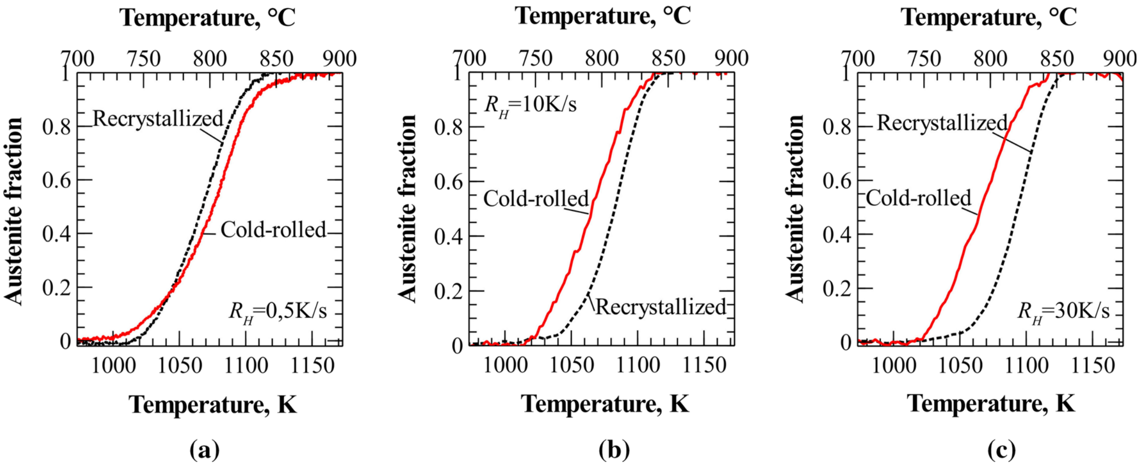

Fig. 3—Comparison of the austenite formation kinetics obtained by dilatometry on the ReX-steel and on the CR-steel during continuous heating with three heating rates: (*a*) $R_H = 0.5$, (*b*) $R_H = 10$, and (*c*) $R_H = 30$ K/s.

$$\frac{dY}{dt} = nk^n t^{n-1}(1-Y) \text{ with } k = k_0 \cdot \exp\left(-\frac{Q}{RT}\right) \quad [1]$$

In relation [1], Y is the transformed fraction ($0 < Y < 1$), n is the Avrami exponent which is usually assumed constant at different temperatures for a given transformation, k_0 is a constant, Q is the activation energy, T is the temperature, and R is the gas constant.

The activation energy associated with the austenite formation kinetics was determined, from the kinetics of Figure 2(a), using the Kissinger analysis developed in the case of non-isothermal treatments.[32] It was thus derived from the slope of the straight line obtained by plotting $\ln\left(\frac{R_H}{T_i^2}\right)$ as a function of $1/T_i$ for different values of the heating rate (R_H). T_i represents, for a given heating rate, the temperature corresponding to the inflection point of the dilatometric curve.

The other parameters of the JMAK law (n, k_0) were adjusted to obtain the best experimental fit. Figure 4 shows the JMAK parametrization of the austenite formation kinetics of the ReX-steel with the following parameters: $Q = 900$ kJ/mol, $n = 0.62$, $k_0 = 6 \times 10^{43}$ s^{-1}. As can be seen, the agreement between the experimental and fitted curves is excellent for the heating rates ranging from 5 to 30 K/s.

It has to be noted that the high value of the activation energy found in this work is in agreement with the values (from 843 to 1155 kJ/mol) which were found by Kulakov *et al.*[4] on a DP600 steel with different initial microstructures (ferrite–pearlite, ferrite–bainite–

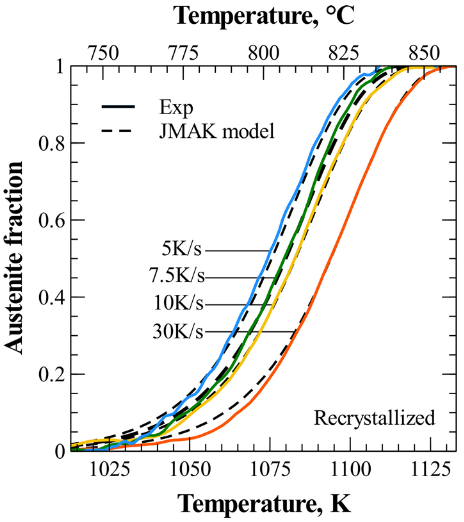

Fig. 4—Comparison between the experimental austenite formation kinetics of the ReX-steel during continuous heating and the JMAK parametrization. The following parameters were used for the JMAK fit: $Q = 900$ kJ/mol, $n = 0.62$, $k_0 = 6 \times 10^{43}$ s^{-1}.

pearlite, martensite). The high value of the determined activation energy for austenite formation has no physical justification. The activation energy of the JMAK law should better be named as "apparent" activation energy.

The preceding approach was also applied in the case of thermal cycles including a heating stage and an isothermal holding at a given annealing temperature (Figure 5). For this study, the experimental austenite formation kinetics was determined by optical microscopy and they were compared with the predictions of the JMAK model. In order to obtain the real fractions during the kinetics, the transformed fractions (Y) given by the JMAK law were multiplied by the local equilibrium (LE) fractions predicted by the Thermo-Calc software.

As can be seen in Figure 5, after an initial increase, the austenite fraction measured at a given annealing temperature tends to stabilize to a maximum value dependant on the temperature. This suggests that the steel has reached an equilibrium at each temperature. In addition, two main points have to be noted: (i) the agreement between theory and experiment is quite good when the local equilibrium fraction is taken into account. This is consistent with the works of Chbihi *et al.*[12] who also highlighted the establishment of a local equilibrium at the ferrite/austenite interface thanks to Mn redistribution; (ii) the heating rate has no strong influence on the austenite formation kinetics and on the final austenite fractions for a given annealing temperature contrary to previous results reported in the literature.[9,12]

C. *Recrystallization Kinetics Without Austenite Formation*

In order to model the recrystallization kinetics of the CR-steel using a JMAK approach, the experimental recrystallization kinetics was determined from the curves given the hardness evolution during isothermal treatments at 923 K, 948 K, and 973 K (650 °C, 675 °C, and 700 °C). From these curves, the evolution of the recrystallized fraction (f_{ReX}) could be plotted as a function of the treatment time at each temperature (Figure 6(a)), taking into account the fact that:

$$f_{\mathrm{ReX}} = \frac{H_0 - H(t)}{H_0 - H_{\mathrm{F}}}, \qquad [2]$$

where H_0, H(t), and H_{F} correspond to the initial hardness (after cold rolling), the hardness after a given time t, at temperature T, and the hardness of the fully recrystallized steel, respectively. The full recrystallization after 1200 seconds at 973 K (700 °C) was confirmed by SEM observation as illustrated in Figure 1(b).

As expected, recrystallization kinetics depends on holding temperature: recrystallization is shifted towards shorter aging times at higher temperature, supporting the occurrence of a thermally activated phenomenon. Therefore, a time–temperature equivalence based on an Arrhenius law with an activation energy Q was used to find the "equivalent time at 923 K (650 °C)" for all aging treatments performed at T and to build a unique master curve. This time–temperature equivalence assumes the same diffusion length for two time–temperature couples (t_{A}, T_{A}) and (t_{B}, T_{B}) and leads to the following equation for the evaluation of the equivalent time at $T_{\mathrm{B}} = 923$ K (650 °C):

$$t_{\mathrm{B}}^{\mathrm{eq}} = \exp\left[\frac{Q}{R}\left(\frac{1}{T_{\mathrm{B}}} - \frac{1}{T_{\mathrm{A}}}\right)\right].t_{\mathrm{A}} \qquad [3]$$

with R being the universal gas constant.

Figure 6(b) shows that the superposition of the curves associated with the three annealing temperatures is very good when an activation energy of 326 kJ/mol is used in Eq. [3]. The use of a unique activation energy in the whole time–temperature domain suggests that a unique mechanism manages the recrystallization phenomenon. Besides, one can note that the obtained value for Q is higher than that associated with the activation energy of 250 kJ/mol determined for self-diffusion in bcc iron. This can be explained by the presence of alloying elements such as Mn which may retard the formation of newly recrystallized grains owing to solute drag on migrating grain boundaries.[9]

Due to the sigmoidal shape of the curves shown in Figure 6(a), the isothermal recrystallization kinetics can be fitted using an isothermal JMAK model expressed by the following relation:

$$Y = 1 - \exp(-(kt)^n) \qquad [4]$$

The activation energy Q was assigned to the previously determined value after time–temperature equivalence. The Avrami coefficient n was obtained by a linearization of the isothermal JMAK law (Eq. [4]) and was found to be equal to 1. Lastly, the third parameter (k_0) was adjusted to obtain the best experimental fit of the experimental recrystallization kinetics with the JMAK law. As can be seen in Figure 6(a), the

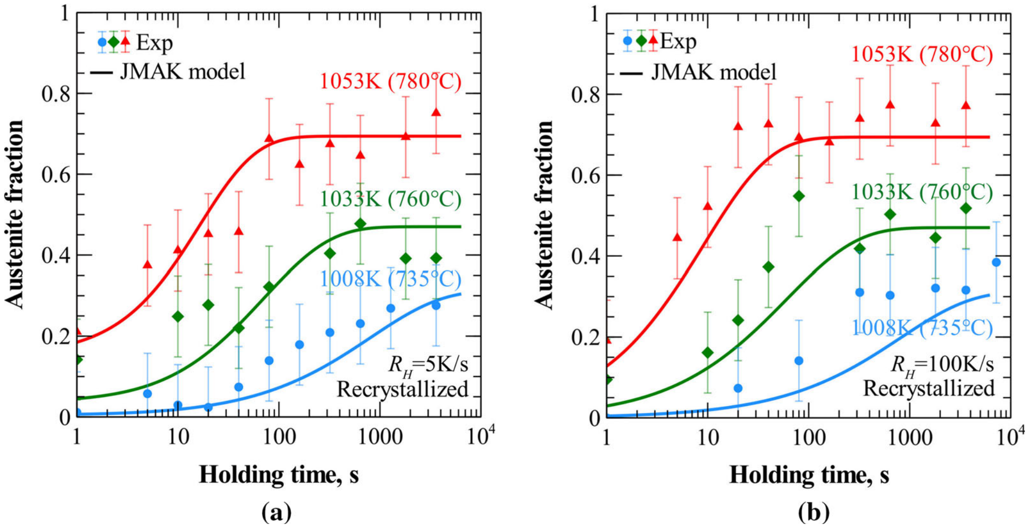

Fig. 5—Comparison between the experimental austenite formation kinetics and the JMAK model for the ReX-steel during isothermal holding at 1008 K, 1033 K, and 1053 K (735 °C, 760 °C, and 780 °C) after a heating ramp with (*a*) $R_H = 5$ and (*b*) $R_H = 100$ K/s. The fractions determined with the JMAK model were calculated considering the local equilibrium condition calculated with Thermo-Calc. The JMAK parameters were determined in continuous heating conditions on the ReX-steel.

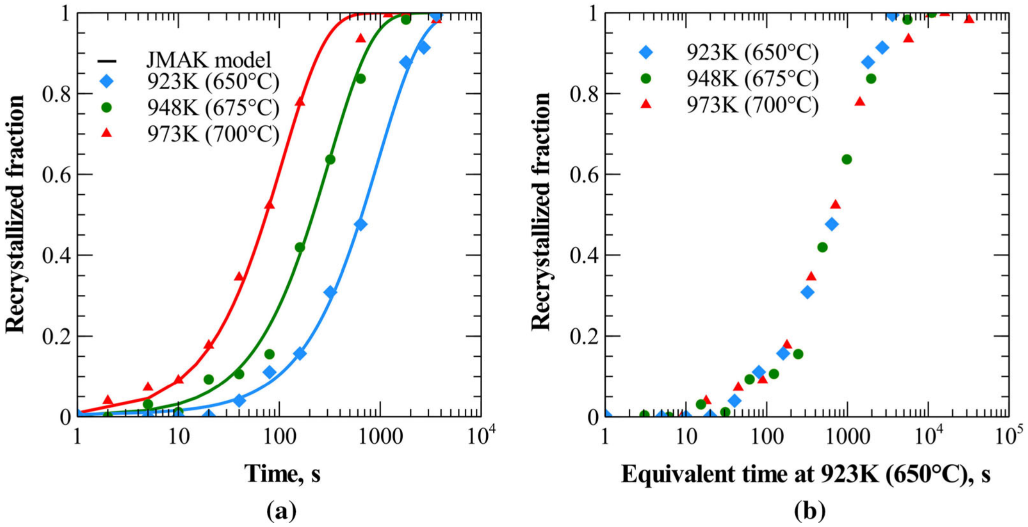

Fig. 6—(*a*) JMAK fit of the experimental data during isothermal holding at 923, 948, and 973K (650 °C, 675 °C, and 700 °C), (*b*) Time–temperature equivalence used to determine the activation energy ($Q = 326$ kJ/mol).

parameters ($Q = 326$ kJ/mol; $n = 1$; $k_0 = 3.0.10^{15}$/s) give very good predictions of the recrystallization kinetics. One can note that the parameters reported in the literature have the same orders of magnitude. Yang *et al.*[3] determined an activation energy that equals to 226 kJ/mol while Huang *et al.*[9] and Li *et al.*[7] found values close to 350 to 380 kJ/mol. These higher values are explained by solute alloying elements generating a solute drag effect on the growth of newly recrystallized grains.

The preceding parametrization, determined from isothermal kinetics, was also used to predict non-isothermal kinetics with the JMAK law in its differential form (Eq. [1]). The model was tested on a complex thermal cycle including a slow heating (with a heating rate of 1 K/s) followed by an isothermal holding at 973 K (700 °C). Figure 7 compares the predicted hardness evolution with that deduced from hardness measurements. The model offers a successful prediction of recrystallization progress.

D. *Interaction Map During Continuous Heating*

The recrystallization model has been used to predict the recrystallization kinetics during continuous heating from room temperature to 1273 K (1000 °C) with a heating rate between 1 and 100 K/s. For each considered heating rate, the recrystallization start temperature (R_{start}) and the recrystallization finish temperature (R_{end}) were determined for a recrystallized fraction of 5 and 95 pct, respectively and were plotted as a function of the heating rate in Figure 8(a).

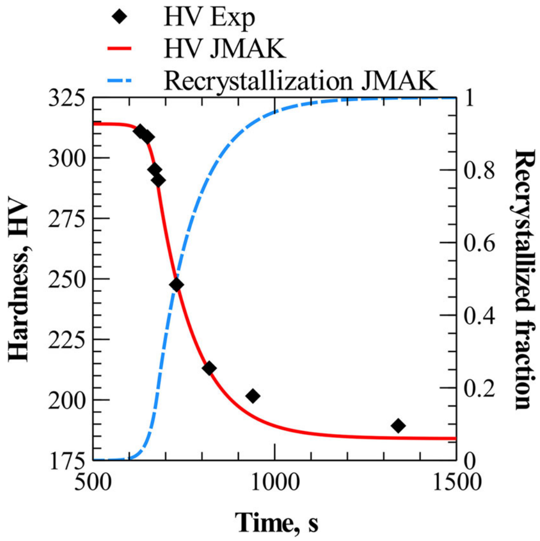

Fig. 7—Experimental and predicted hardness evolution during a complex cycle [heating at 1 K/s, then holding at 973 K (700 °C)] validating the JMAK model for recrystallization.

The austenite formation domain associated with the ReX-steel and with the CR-steel has been added, leading to a map of phenomena occurring during non-isothermal intercritical annealing. The austenite formation domain of each steel was built from the austenite start temperature (A_{C1}) and the austenite finish temperature (A_{C3}) deduced from the dilatometric curves of Figure 2.

Several conclusions can be drawn from the map of Figure 8(a). First, recrystallization is not finished when the austenite start temperature is reached for all heating rates in between 1 and 100 K/s. This indicates the occurrence of a wide temperature domain for which recrystallization and austenite formation overlap and can potentially interact. Second, the map of Figure 8(a) clearly shows that austenite starts to form without any recrystallization of the system when the heating rate is higher than 30 K/s. In these conditions, the energy stored during the cold-rolling step is expected to be a supplementary driving force for the austenite formation. Lastly, it has to be noted that for heating rates higher than 15 K/s, recrystallization predicted by the model is not finished while austenite has finished to form. Indeed, the recrystallization model does not consider the phase transformation and assumes that the recrystallization kinetics is not affected by austenite formation. This seems to be effectively the case for austenite fractions lower than 10 pct because of limited ferrite–austenite interfaces, as suggested by Ogawa *et al.*[13] However, when austenite fraction is larger than 30 pct, recrystallization could be considerably delayed[10] or even suppressed,[14] limiting the recrystallization model above A_{C1}.

To complete this work, the recrystallized fraction at the austenite start temperature was plotted as a function of the heating rate in Figure 8(b). The decrease in the recrystallized fraction at Ac_1 appears to be very abrupt for heating rates lower than 1 K/s. For heating rates superior to 1 K/s, recrystallized fractions are lower than 30 pct. In other words, recrystallization is just at its beginning when austenite starts to form.

E. *Austenite Formation Kinetics with Recrystallization*

In the case of the CR-steel, austenite formation is likely to occur either in a fully recrystallized matrix at very slow heating rates ($R_H < 0.5$ K/s) or in a matrix combining a mixture of recrystallized ferrite grains and of deformed grains at intermediate and high heating rates. This leads to a rather complex dependence of the austenite formation kinetics with the heating rate, as was highlighted on the non-isothermal austenite formation kinetics of Figure 2(b).

This observation can be explained by the fact that the austenite formation kinetics is very different in the deformed and recrystallized ferrite grains, as suggested by the results of Figure 3 which support the hypothesis that austenite formation is accelerated when deformed ferrite grains are present in the microstructure. Namely, the energy stored in the deformed ferrite grains during cold rolling could increase the driving force for the transformation.[12]

In order to model the non-isothermal austenite formation kinetics of the CR-steel shown in Figure 3(b), a mixture law taking into account the evolution of the fraction of recrystallized grains during the treatment was employed. The austenite formation kinetics of the CR-steel, f_γ, during a given treatment was thus expressed by the following relation:

$$f_\gamma = f_\alpha^{\mathrm{ReX}} f_\gamma^{\mathrm{ReX}} + (1 - f_\alpha^{\mathrm{ReX}}) f_\gamma^{\mathrm{CR}}, \qquad [5]$$

where f_α^{ReX} represents the recrystallization kinetics of the steel (determined in Section III–C), f_γ^{ReX} is the austenite formation kinetics in the recrystallized ferrite grains (determined in Section III–B), and f_γ^{CR} is the austenite formation kinetics in the deformed ferrite grains.

In the present work, two different JMAK laws were associated with the austenite formation kinetics in the recrystallized and non-recrystallized ferrite grains. They were characterized by the same values of Q and n but by a different value of k_0. A higher value of this parameter was assigned to the JMAK law associated with the austenite formation in deformed ferrite grains to take into account the acceleration of the kinetics. This value was adjusted to obtain the best fit of the experimental data at the very beginning of the austenite formation kinetics. Table II summarizes the parameters of the three JMAK laws used in the mixture law presented above.

Figure 9(a) shows the austenite formation kinetics predicted by the mixture law during continuous heating of the CR-steel with a heating rate of 30 K/s and the different components of the law (*i.e.*, recrystallization kinetics, austenite formation kinetics in recrystallized ferrite grains or in deformed ferrite grains). The agreement between experiment and theory is good for austenite fractions lower than 0.3. Below this fraction, the kinetics is mainly controlled by the deformed ferrite grains, the proportion of which is much higher than that

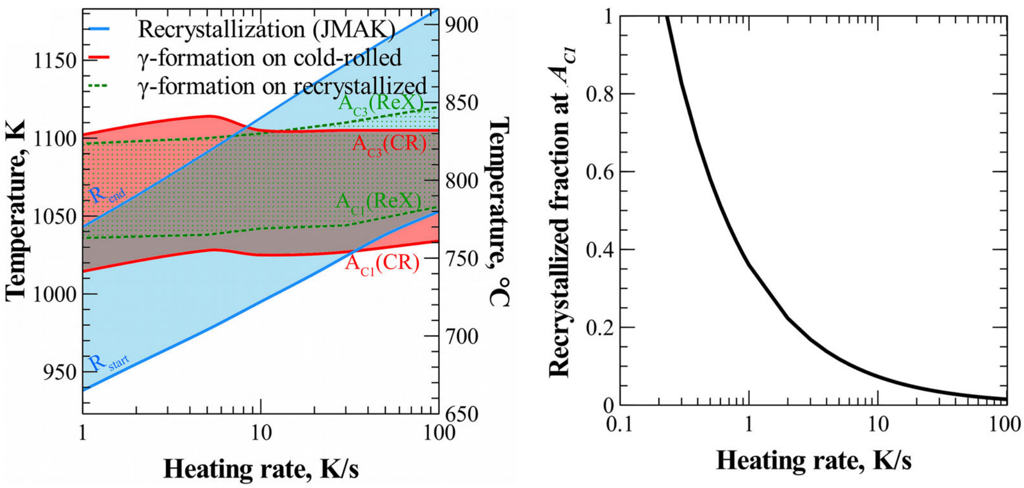

(a) (b)

Fig. 8—(*a*) Interaction map between recrystallization (blue area) and austenite formation (red) in non-isothermal condition; (*b*) Evolution of the recrystallized fraction at Ac_1 temperature as a function of the heating rate.

Table II. JMAK Parameters for Recrystallization and for Austenite Formation Kinetics in Recrystallized Ferrite or in Deformed Ferrite

Phenomena	Q (kJ/mol)	n	k_0 (s^{-1})
Recrystallization	326	1	3E + 15
Austenite formation in recrystallized ferrite	900	0.62	6E + 43
Austenite formation in deformed ferrite	900	0.62	3E + 45

of the recrystallized ferrite grains. At higher austenite fractions, the model predicts a slower kinetics than the experimental one. This is due to the fact that the model considers that the fraction of recrystallized grains gradually increases during heating and that the recrystallization kinetics is not influenced by austenite formation. This is contrary to the observations of References 13 and 14 which showed that the recrystallization kinetics could be considerably retarded above a critical austenite fraction. In order to check this hypothesis, the mixture law was used considering that recrystallization is blocked when the austenite fraction exceeds 10 pct (Figure 9(b)). This gives a much better prediction of the austenite formation kinetics and supports the fact that recrystallization could be effectively inhibited above a critical austenite fraction as mentioned in the introduction of this paper (which refers to the works of Chbihi *et al.* and Barbier *et al.*[12,14]).

The mixture law was also applied to predict the austenite formation kinetics of the CR-steel during thermal cycles including a heating stage (R_H = 5 K/s) and an isothermal holding at a given annealing temperature [between 993 K and 1053 K (720 °C and 780 °C)]. Figure 10(a) shows the experimental and predicted austenite fractions obtained in two cases: (i) without taking into account the inhibition of recrystallization and (ii) with recrystallization inhibition above a critical austenite fraction of 10 pct. As for the ReX-steel, the austenite fractions given by the mixture law were calculated considering the Thermo-Calc local equilibrium conditions. Furthermore, the end of the recrystallization predicted by the JMAK model (presented in Section III–C) was marked by a star item on the curves of Figure 10(a).

As can be seen in Figure 10(a), at all temperatures, austenite fractions increase before reaching a plateau, suggesting the achievement of an apparent equilibrium. At low temperatures [993 K and 1008 K (720 °C and 735 °C)], austenite fractions are rather well predicted for all annealing times. For these two temperatures, recrystallization inhibition has no influence on the kinetics, since recrystallization is completed before reaching the critical austenite fraction for which recrystallization is blocked. For the intermediate temperature [1033 K (760 °C)] and the highest temperature [1053 K (780 °C)], a better agreement between experiment and theory is obtained if recrystallization inhibition is taken into account. Namely, at these two temperatures, recrystallization and austenite formation occur simultaneously and this greatly influences the austenite formation kinetics. However, a significant difference can be noted on the values of the equilibrium austenite fractions at 1033 K and 1053 K (760 °C and 780 °C). At 1033 K (760 °C), the experimental fraction (around, 40 pct) is in good agreement with the local equilibrium fraction given by Thermo-Calc. This is not the case at 1053 K (780 °C) where the experimental fraction on the plateau (about 88 pct) is much higher than the local equilibrium fraction (66 pct). This unexpected result will be discussed further in Section IV–B–2.

Lastly, Figure 10(b) presents the effect of the heating rate on the austenite formation kinetics of the CR-steel at 1033 K (760 °C). Increasing the heating rate from 5 to 30 K/s leads to a marked acceleration of the kinetics. This can be explained by the delay of recrystallization when heating rate is increased. The model captures this

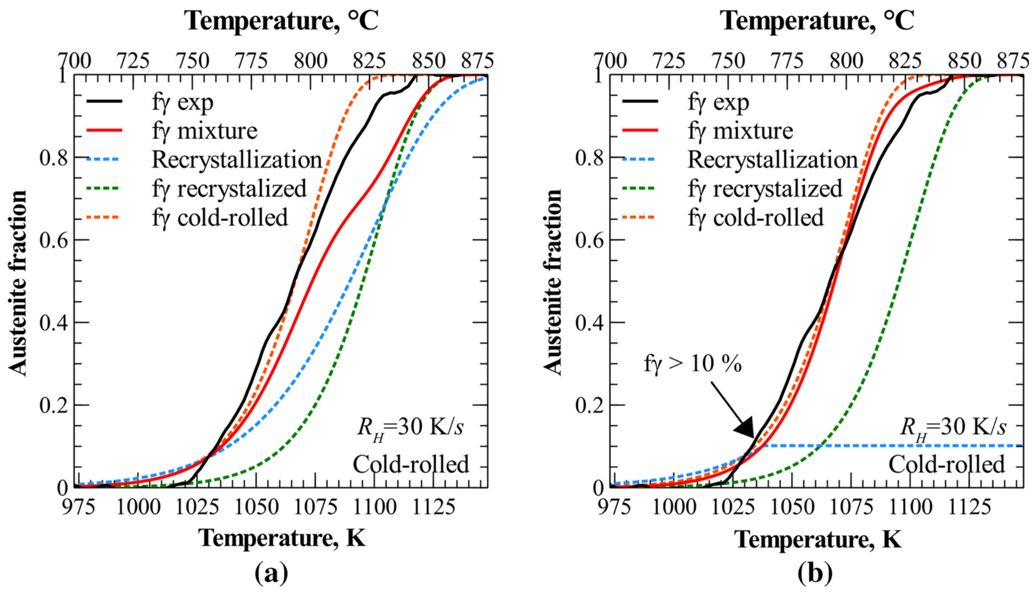

Fig. 9—Comparison between the experimental austenite formation kinetics of the CR-steel and the theoretical kinetics based on a mixture law during continuous heating at 30 K/s: (*a*) without recrystallization inhibition; (*b*) with recrystallization inhibition for austenite fractions higher than 10 pct. The different components of the mixture law were reported in dash points.

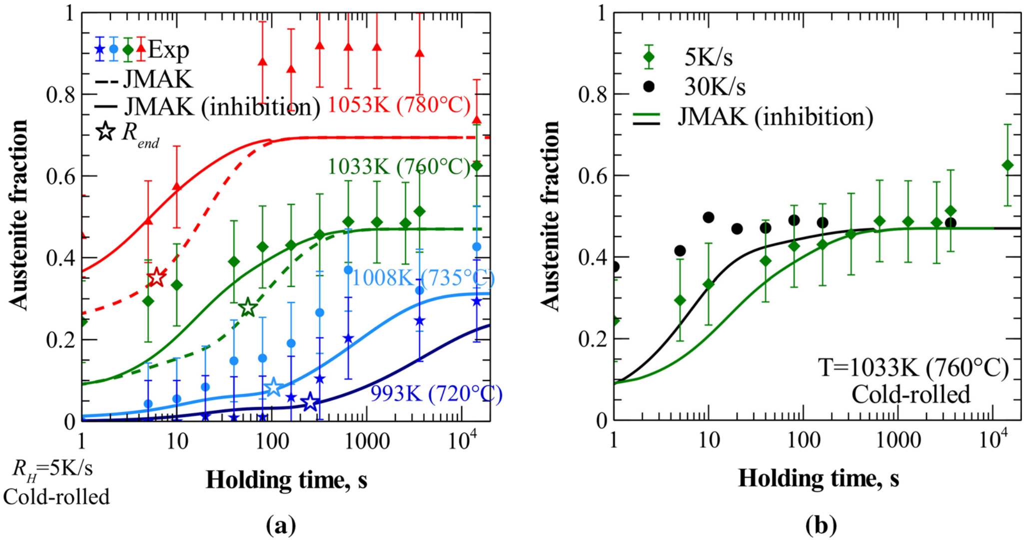

Fig. 10—(*a*) Comparison between the experimental austenite formation kinetics of the CR-steel and the theoretical kinetics based on a mixture law during isothermal holding at 993 K, 1008 K, 1033 K, and 1053 K (720 °C, 735 °C, 760 °C, and 780 °C) after a heating stage with R_H = 5 K/s. The stars correspond to the end of recrystallization and solid lines consider recrystallization inhibition below 10 pct of austenite fraction. (*b*) Effect of the heating rate on the experimental and modeled austenite formation kinetics during isothermal holding at 1033 K (760 °C).

acceleration of the kinetics but it is slightly retarded compared to experimental kinetics during the first ten seconds of holding.

IV. DISCUSSION

The aim of this section is to discuss and analyze the influence of several parameters (initial state of the steel, annealing temperature, heating rate) considered in this work. Strength and weakness of the proposed model based on a combination of 3 JMAK laws are discussed in a final section.

A. *Influence of the Initial State on the Austenite Formation Kinetics*

The results presented in the preliminary work of this paper (Section III–A, Figure 3) clearly showed that the austenite formation kinetics of the CR-steel is: (i) identical to that of the ReX-steel at low heating rate (R_H = 0.5 K/s) and (ii) tends to be accelerated compared to that of the ReX-steel at higher heating rates, all the more as the heating rate is high.

These observations can be explained by two main effects: (1) the presence of non-recrystallized ferrite grains in the CR-steel could promote the austenite

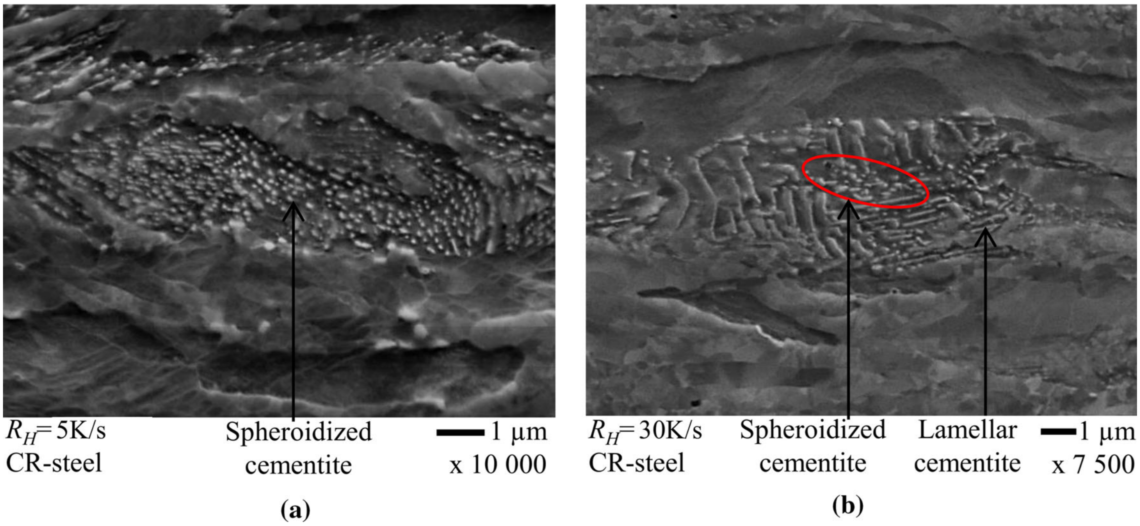

Fig. 11—SEM observations of microstructural states of a cold-rolled steel after heating at (*a*) 5 and (*b*) 30 K/s to 993 K (720 °C). A full spheroidization of cementite is observed after 5 K/s while spheroidization is rather partial with 30 K/s heating rate.

nucleation by increasing the driving force for the austenite formation and accelerate the kinetics of the CR-steel[4,12]; (2) the cementite spheroidization highlighted by the SEM observations of the initial microstructure of the ReX-steel could be responsible for a delay in austenite nucleation and retard the kinetics of the ReX-steel.[7]

In order to analyze these two effects and to identify their respective roles on the austenite formation kinetics, the evolution of cementite morphology during the heating stage of the CR-steel was analyzed by SEM observations before austenite nucleation (Figure 11). To this end, the CR-steel was heated up to 993 K (720 °C) with two heating rates (5 and 30 K/s) and subsequently, water quenched. As can be seen in Figure 11, cementite spheroidization occurs very rapidly during the heating stage. For the lower heating rate, cementite spheroidization is total and relatively similar to that of the ReX-steel, while it is only partial at the higher heating rate. These results tend to indicate that the effect of cementite spheroidization may play a role on the austenite kinetics but it should not be predominant. Namely, cementite spheroidization takes place very rapidly during the heating stage of the CR-steel and austenite nucleation is expected to occur mainly from spheroidized cementite both in the CR-steel and in the ReX-steel (especially for heating rates lower than 5 K/s).

In these conditions, the degree of recrystallization of the ferrite matrix before austenite formation seems to be the major parameter to consider, in view of understanding the austenite formation kinetics. For a heating rate of 0.5 K/s, the kinetics of austenite formation are identical for the ReX-steel and for the CR-steel, as recrystallization has largely occurred in the CR-steel before austenite formation (as can be deduced from the results of Figure 8(b)). Such behavior was also observed by Azizi-Alizamini *et al.*[2] for a heating rate of 1 K/s. Authors also explained that this is due to the fact that recrystallization of ferrite in the cold-rolled steel takes place before austenite formation. In the case of higher heating rates, recrystallization is just at its very beginning when austenite starts to form and this tends to accelerate strongly the austenite formation kinetics.

B. *Influence of the Temperature and of the Heating Rate on the Austenite Formation Kinetics*

1. *Case of the ReX-steel*

When the temperature is increased, the austenite formation kinetics is accelerated and the equilibrium austenite fractions increase. Moreover, the equilibrium fractions obtained at each temperature are in agreement with those given by Thermo-Calc under local equilibrium conditions. These observations are in perfect accordance with those of Chbihi *et al.*[12] for the description of the metastable equilibrium obtained for short treatment times. They support the fact that the orthoequilibrium is not reached in typical industrial conditions. This was also pointed out by the works of Lai *et al.*[22] who estimated the time to reach the orthoequilibrium to be of the order of 10^6 seconds [at 1013 K (740 °C)] with DICTRA software. Lastly, it has to be emphasized that the assumption of paraequilibrium does not describe the equilibrium condition. The difference in the composition of the substitutional elements, such as Mn, in the two initial phases (*i.e.,* ferrite and cementite) could explain the fact that the paraequilibrium condition is not verified in the case of the investigated steel. Indeed, the gradient of composition could promote local diffusion through the interface despite the slow diffusivities of Mn and generate a LE condition.

Furthermore heating rate does not influence the equilibrium austenite fraction at a given temperature. In addition, it has no strong influence on the austenite formation kinetics (Figure 5). This is particularly true when no austenite formed during the heating stage or when the austenite fraction formed during heating is low (that is to say at low annealing temperature). This is illustrated in Figure 12(a) for an annealing at 1033 K

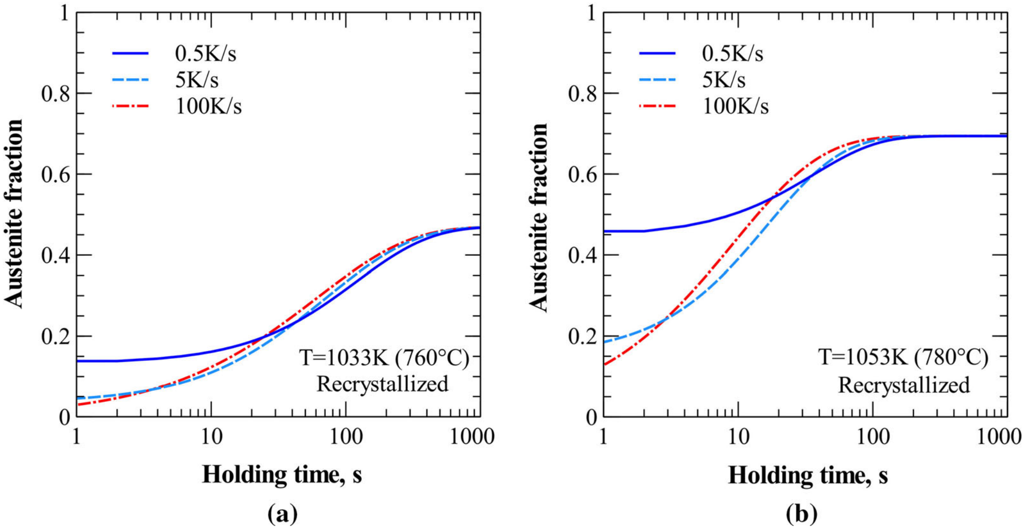

Fig. 12—Effect of the heating rate R_H on the austenite kinetics during isothermal holding at (*a*) 1033 K and (*b*) 1053 K (760 °C and 780 °C) of a prior recrystallized steel. The kinetics was predicted using the JMAK model defined in Section III–B.

(760 °C). No effect of the heating rate is noted when this parameter passes from 5 to 100 K/s, since no austenite formed during the heating stage. However, a little effect is observed when the heating varies between 0.5 and 100 K/s due to the formation of a low austenite fraction during heating with $R_H = 0.5$ K/s. At higher annealing temperature [1053 K (780 °C)], the effect of the heating rate is more marked, as shown in Figure 12(b).

It has to be noted that the low influence of the heating rate found in this work for the ReX-steel is not in agreement with the results of Huang *et al.*[9]. These authors observed that the austenite formation kinetics obtained at 1023 K (750 °C) on a hot-rolled Fe-C-Mn-Mo steel was different after a slow heating (1 K/s) or after a rapid heating (100 K/s). In particular, they noted that the measured austenite fractions were much lower when the heating rate was slow without providing any physically based argument. Chbihi *et al.*[12] obtained also the same conclusions. However, it has to be mentioned that their results concern short treatment times at 1013 K (740 °C) (less than 600 seconds) for which no equilibrium is reached.

2. *Case of the CR-steel*

In the case of the CR-steel, the effect of the heating rate and of the temperature is more difficult to analyze due to the interaction between recrystallization and austenite formation. Depending on the parameters of the cycles, this interaction can be weak (at low temperature and low heating rate) or strong (at high temperature and high heating rate).[12,14]

For a weak interaction, recrystallization occurs mainly before austenite formation, so that the austenite formation kinetics is similar to that determined for the ReX-steel. For the investigated steel, a weak interaction was observed at low temperature [993 K and 1008 K (720 °C and 735 °C)] with $R_H = 5$ K/s as shown in Figure 10(a). At these two temperatures, recrystallization is finished before 10 pct of austenite has formed.

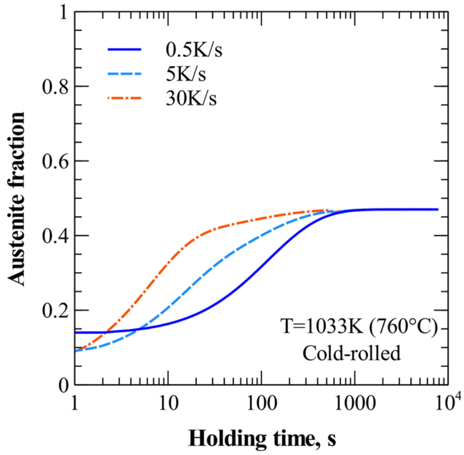

Fig. 13—Effect of the heating rate R_H on the austenite kinetics during isothermal holding at 1033 K (760 °C) of a cold-rolled steel. The kinetics was predicted using the mixture law with recrystallization inhibition defined in Section III–E.

For a strong interaction obtained at higher temperatures, recrystallization and austenite formation are concomitant. This experimental fact has two main consequences.

The first consequence is that the effect of the heating rate is much more marked than in the ReX-steel. This is illustrated in Figure 13, where the austenite formation kinetics during isothermal holding at 1033 K (760 °C) was predicted, for three different heating rates, using the mixture law (with recrystallization inhibition) as defined in Section III–E. Figure 13 highlights that increasing the heating rate strongly accelerates the austenite formation kinetics, contrary to the case of the ReX-steel presented in Figure 12(a) at the same temperature. This acceleration can be attributed to the fact that the proportion of non-recrystallized ferrite grains at the austenite start temperature (Figure 8(b)) is higher at high heating rate (respectively estimated to be equal to 1, 53, and 82 pct at

Table III. Comparison of Thermo-Calc and Experimental Austenite Fraction on CR-Steel After 1 and 4 h of Isothermal Holding

Austenite Fraction	993 K (720 °C)	1008 K (735 °C)	1033 K (760 °C)	1053 K (780 °C)
Experimental after 1 h of isothermal holding	0.24	0.32	0.50	0.88
Experimental after 4 h of isothermal holding	0.29	0.42	0.62	0.73
ORTHO FeCMnCrSiAl	0.34	0.40	0.54	0.70
LE FeCMn	0.24	0.31	0.46	0.66

the beginning of the isothermal holding for 0.5, 5, and 30 K/s heating rates). This is due to the shift of the recrystallization kinetics towards higher temperatures and to recrystallization inhibition. These two phenomena lead to an increase of the fraction of deformed ferrite grains on which austenite nucleates and to an acceleration of the austenite formation kinetics.

The second consequence of the interaction is that the equilibrium austenite fraction obtained after annealing at high temperature cannot be predicted using the local equilibrium fractions given by Thermo-Calc. This was observed in Figure 10(a) in the case of the kinetics at 1053 K (780 °C), where the combination of a high annealing temperature and of a high fraction of deformed ferrite grains probably promote the diffusion of the alloying elements of the steel. Namely, the dislocations of the ferrite matrix could provide favorable diffusion paths for Mn[4,12] and thus reach an intermediate state between LE and ORTHO equilibria for times inferior to 100 seconds. Note that this intermediate state contains more austenite than both LE and ORTHO as shown by Wei *et al.*[24] and Lai *et al.*[22] The transition between LE to ORTHO seems to be also highlighted at the other holding temperatures for long treatment times (4 hours) as reported in Table III. Table III compares experimental austenite fractions measured after 1 and 4 hours of holding with the ORTHO and LE fractions. For all temperatures in between 993 K and 1033 K (720 °C and 760 °C), the austenite fractions evolve and increase between 1 and 4 hours of holding remaining the "Mn-diffusion in ferrite" regime before reaching the ORTHO equilibrium.[22,24]

C. *Pragmatic Tool for Microstructural Evolutions During Intercritical Annealing*

The present paper proposes an original modeling tool allowing the microstructural evolutions occurring during complex intercritical annealing treatments to be described. Based on the combination of three JMAK laws, the model enables to describe the evolution of the recrystallization and of the austenite formation of cold-rolled DP steels. Austenite formation is treated differentiating two types of kinetics for the two considered nucleation sites (*i.e.*, deformed and recrystallized ferrite grains). These two contributions are then linked in a mixture law taking into account the recrystallization progress.

This tool also ensures to implement, for the first time, the recrystallization inhibition above a critical austenite fraction (of the order of 10 pct) which has been suggested in the literature by different authors.[12,14] As was shown in the present paper, the implementation of this phenomenon leads to a better description of the austenite formation kinetics above the critical austenite fraction. In particular, the acceleration of the kinetics resulting from recrystallization inhibition was found to be in good agreement with the experimental results both in non-isothermal and isothermal conditions.

To our knowledge, the developed approach is innovative not only by the distinction of the two sites for austenite formation but also by the simple implementation of the recrystallization inhibition on to suppress empirical laws.

Such model is likely to predict the effect of several parameters of the thermal cycles (heating rate, annealing temperature, and annealing time) on the microstructural evolutions of cold-rolled DP steels. It is a pragmatic tool that could be used as an online production tool to predict the microstructure modifications and even to optimize thermal treatments.

However, as JMAK laws are based on a phenomenological equation, the parameters of these laws may depend both on the steel chemistry and on the reduction ratio of the steel sheets. The proposed model is thus not directly transposable to all types of DP steels but a similar approach could be used to adjust model parameters.

V. CONCLUSIONS

The present paper deals with the experimental characterization and the modeling of the austenite formation kinetics of a DP1000 steel with an initial ferrite–pearlite microstructure (either fully recrystallized or cold-rolled). For the experimental study, dilatometric and optical microscopy measurements were used to follow the kinetics of austenite formation during different types of thermal cycles. For the modeling, simple JMAK laws were used to describe the recrystallization kinetics without austenite formation and the austenite formation kinetics without recrystallization. To study the complex case of the cold-rolled steel for which austenite formation and recrystallization are expected to occur simultaneously, a mixture law was employed. The influence of several parameters (initial state of the steel, annealing temperature, heating rate) on the austenite formation kinetics was discussed.

1. In the case of the ReX-steel, the austenite formation kinetics could be successfully described by a simple JMAK law with the following parameters : Q = 900 kJ/mol, n = 0.62, and k_0 = 6.10^{43} s^{-1}. Using the local equilibrium fractions given by Thermo-Calc, the isothermal austenite formation kinetics of the ReX-steel could be successfully modeled for

treatment times from 1 seconds to 1 hour. Moreover, no strong influence of the heating rate was found on the austenite formation kinetics and on the final austenite fractions, contrary to previous results of the literature.

2. The recrystallization kinetics of the steel without austenite formation was modeled by a JMAK law with the following parameters : $Q = 325$ kJ/mol, $n = 1$, and $k_0 = 3 \times 10^{15}$ s^{-1}. Using this model during continuous heating with different heating rates, an interaction map between recrystallization and austenite formation could be built. It highlighted that the degree of recrystallization before austenite formation depends strongly on the heating rate and is less than 30 pct for heating rates higher than 1 K/s.
3. A simple mixture law was used to describe the austenite formation kinetics of the CR-steel under various conditions. It was based on the assumption that two different JMAK laws are necessary to describe austenite nucleation in the recrystallized ferrite grains and in the deformed ferrite grains. The results presented in this paper showed that the experimental curves are well fitted in the case of a weak interaction between recrystallization and austenite formation. For a strong interaction (high temperature, high heating rate), the curves are better fitted by the model when recrystallization is inhibited above a critical austenite fraction, supporting the results of several studies.[13,14]
4. In the case of the CR-steel, a strong influence of the heating rate was noted on the austenite formation kinetics when a strong interaction is expected, due to the marked dependence of the recrystallized fraction at the austenite start temperature with this parameter. In addition, it was suggested that the combination of a high temperature and a high deformed structure tends to accelerate the diffusion of the alloying elements in the steel. In these conditions, the final austenite fractions obtained at high temperature cannot be described using the local equilibrium fractions given by Thermo-Calc.
5. Lastly, the present work showed that the acceleration of the austenite formation kinetics in the CR-steel compared to the kinetics of the ReX-steel can be mainly explained by the degree of recrystallization before austenite formation and, partly, by cementite spheroidization which may occur during heating. For usual industrial heating rates, the recrystallized fraction of the CR-steel is low at the A_{C1} temperature, which tends to promote austenite nucleation in the deformed ferrite grains and to accelerate the transformation kinetics.

ACKNOWLEDGMENTS

This work was carried out in collaboration with the Fives Keods company which is attaching great importance to physical modeling in order to improve the efficiency of his line driving softwares. Authors thank this company for the financial support. M. Gouné and M. Militzer are also gratefully acknowledged for fruitful discussions.

REFERENCES

1. R.O. Rocha, T.M.F. Melo, E.V. Pereloma, and D.B. Santos: *Mater. Sci. Eng. A*, 2005, vol. 391, pp. 296–304.
2. H. Azizi-Alizamini, M. Militzer, and W.J. Poole: *Metall. Mater. Trans. A*, 2011, vol. 42A, pp. 1544–57.
3. D.Z. Yang, E.L. Brown, D.K. Matlock, and G. Krauss: *Metall. Trans. A*, 1985, vol. 16A, pp. 1385–92.
4. M. Kulakov, W.J. Poole, and M. Militzer: *Metall. Mater. Trans. A*, 2013, vol. 44A, pp. 3564–76.
5. E.A. Chojnowski and W.J.Mc.G. Tegart: *Met. Sci. J.*, 1968, vol. 2, pp. 14–18.
6. D.F. Lupton and D.H. Warrington: *Met. Sci. J.*, 1972, vol. 6, pp. 200–04.
7. P. Li, J. Li, Q. Meng, W. Hu, and D. Xu: *J. Alloys Compds.*, 2013, vol. 578, pp. 320–27.
8. G.R. Speich, V.A. Demarest, and R.L. Miller: *Metall. Trans. A*, 1981, vol. 12A, pp. 1419–28.
9. J. Huang, W.J. Poole, and M. Militzer: *Metall. Mater. Trans. A*, 2004, vol. 35A, pp. 3363–75.
10. T. Ogawa, N. Maruyama, N. Sugiura, and N. Yoshinaga: *ISIJ Int.*, 2010, vol. 50, pp. 469–75.
11. R.R. Mohanty, O.A. Girina, and N.M. Fonstein: *Metall. Mater. Trans. A*, 2011, vol. 42A, pp. 3680–90.
12. A. Chbihi, D. Barbier, L. Germain, A. Hazotte, and M. Gouné: *J. Mater. Sci.*, 2014, vol. 49, pp. 3608–21.
13. T. Ogawa: *International Journal of Mechanical and Materials Engineering*, 2015.
14. D. Barbier, L. Germain, A. Hazotte, M. Gouné, and A. Chbihi: *J. Mater. Sci.*, 2015, vol. 50, pp. 374–81.
15. C. Zheng and D. Raabe: *Acta Mater.*, 2013, vol. 61, pp. 5504–17.
16. J. Rudnizki, B. Bottger, U. Prahl, and W. Bleck: *Metall. Mater. Trans. A*, 2011, vol. 42A, pp. 2516–25.
17. M. Kulakov, W.J. Poole, and M. Militzer: *ISIJ Int.*, 2014, vol. 54, pp. 2627–36.
18. https://www.gleeble.com/products/gleeble-3500.html.
19. https://imagej.net.
20. J.O. Andersson, T. Helander, L. Hoglund, P.F. Shi, and B. Sundman: *Comput. Tools Mater. Sci. Calphad*, 2002, vol. 26, pp. 273–312.
21. Thermo-Calc software TCFE8 Steels/Fe-alloys database version 8 (accessed 23 July 2016).
22. Q. Lai, M. Gouné, A. Pierlade, T. Pardoen, P. Jacques, O. Bouaziz, and Y. Bréchet: *Metall. Mater. Trans. A*, 2016, vol. 47A, pp. 3375–86.
23. A. Hultgren: *Trans. Am. Soc. Met.*, 1947, vol. 39, pp. 915–1005.
24. R. Wei, N. Enomoto, R. Hadian, H.S. Zurob, and G.R. Purdy: *Acta Mater.*, 2013, vol. 61, pp. 697–707.
25. H. Chen, X. Xu, W. Xu, and S. van der Zwaag: *Metall. Mater. Trans. A*, 2014, vol. 45A, pp. 1675–79.
26. H.S. Zurob, C.R. Hutchinson, Y. Bréchet, H. Seyedrezai, and G.R. Purdy: *Acta Mater.*, 2009, vol. 57, pp. 2781–92.
27. M. Gouné, F. Danoix, J. Ågren, Y. Bréchet, C.R. Hutchinson, M. Militzer, G. Purdy, S. Van der Zwaag, and H. Zurob: *Mater. Sci. Eng.*, 2015, vol. 92, pp. 1–38.
28. T. Ogawa, K. Sato, H. Dannoshita, K. Maruoka, and K. Ushioda: *ISIJ Int.*, 2016, vol. 5, pp. 2290–97.
29. M. Avrami: *J. Chem. Phys.*, 1939, vol. 7, p. 1103.
30. W.A. Johnson and R.F. Mehl: *Trans. Am. Inst. Min. Metall. Pet. Eng.*, 1939, vol. 135, p. 416.
31. A. Kolmogorov: *Izv. Acad. Sci. USSR, Math. Ser.*, 1937, vol. 1, p. 355.
32. H. Kissinger: *Anal. Chem.*, 1957, vol. 29, pp. 1702–06.